ARTICLES

Two-Dimensional Polymers Investigated by Scanning Near-Field Optical Microscopy: Phase Separation of Polymer Blend Monolayer

Hiroyuki Aoki and Shinzaburo Ito*

Department of Polymer Chemistry, Graduate School of Engineering, Kyoto University, Sakyo, Kyoto 606-8501, Japan

Received: September 13, 2000; In Final Form: February 5, 2001

Scanning near-field optical microscopy (SNOM) was employed for investigating the phase separation behavior of a polymer blend monolayer which consisted of dye-labeled poly(octadecyl methacrylate) (PODMA) and poly(isobutyl methacrylate) (PiBMA), both forming stable monolayers at the air/water interface. The energy transfer emission was observed in the PODMA rich domain, indicating that there existed the area where both components were mixed at the molecular level. When the polymer blend solution is spread onto a water surface, the PODMA chains tend to aggregate and form a solidlike domain before the PODMA and PiBMA separate completely from each other. This is attributed to the strong crystallinity of the long alkyl group of PODMA. When the temperature was raised to 40 °C, the phase separation was almost completed in several minutes, and then the domain size increased with annealing time. The two-dimensional structure for the completely phase-separated monolayer was studied by time-resolved SNOM. A near-field fluorescence decay was observed across the phase interface. The alteration of the fluorescence lifetime at the phase boundary indicated that the interfacial width for the two-dimensionally phase-separated polymer blend was markedly larger than the interfacial thickness expected in three dimensions.

Introduction

A variety of amphiphilic polymers are known to form monolayers at the air/water interface. Sequential deposition of the monolayer allows one to construct well-defined layered structures in a nanometric scale.[1−4] The polymer chains in a monolayer are expected to have properties different from those in a three-dimensional space[5−7] because of the low degree of freedom for the chains restricted in a two-dimensional plane. Although the understanding of properties and morphology of polymer monolayers is important in fabricating well-defined assemblies, we have little knowledge on the polymers in two-dimensional systems. Our research project is concerned with the phase separation of polymer blend monolayers, which has attracted potential interests from the viewpoints of not only polymer physics in two dimensions but also application as a self-organizing method[8,9] to control the in-plane structure of nanofabrics.

Direct observation of the two-dimensional morphology of polymer monolayers has been carried out so far by Brewster angle microscopy (BAM)[6,10,11] and atomic force microscopy (AFM).[9,11,12] Recently, scanning near-field optical microscopy (SNOM) has attracted much attention from researchers in various fields. SNOM is an emerging scanning probe microscopic technique, which illuminates a specimen with the optical near field emanating from an aperture much smaller than the wavelength of light.[13−16] Since SNOM uses "light" as a probe, spectroscopic and time-resolved measurements are applicable to a nanometric local area. This allows one to obtain various unique information, such as the molecular orientation and the chemical composition of the specimen, with a subwavelength spatial resolution. SNOM is expected to be a powerful tool in investigating the two-dimensional morphology of polymer monolayers as well as the other organic systems: lipid monolayers,[17,18] self-assembled films,[19] liquid crystals,[20] and dye aggregates.[21,22]

The previous study examined the phase separation process of a blend monolayer consisting of poly(octadecyl methacrylate) (PODMA) and poly(isobutyl methacrylate) (PiBMA) by using BAM and AFM.[11] It showed that the morphology of the PODMA/PiBMA mixed monolayer was changed by raising the temperature of the subphase; however, BAM and AFM could not probe the coexisting state of both polymers at the molecular level. In the earlier letter,[23] the phase separation structure of a polymer blend monolayer was examined by fluorescence SNOM. For the completely phase-separated monolayer, the phase boundary region could be selectively visualized in the SNOM image by the energy transfer emission from the region where both components were molecularly mixed. In the present paper, the phase separation behavior of the dye-labeled PODMA/PiBMA blend monolayers was studied in more detail by means of SNOM. The two-dimensional morphology was examined through the energy transfer emission mapping with SNOM. The time-resolved measurements in the near field were also carried out for the phase-separated monolayers with a temporal resolution of subnanoseconds. The phase separation structure before

* Corresponding author. Phone:+81-75-753-5612. Fax:+81-75-753-5632. E-mail:sito@polym.kyoto-u.ac.jp.

10.1021/jp0032412 CCC: $20.00
Published on Web 04/07/2001

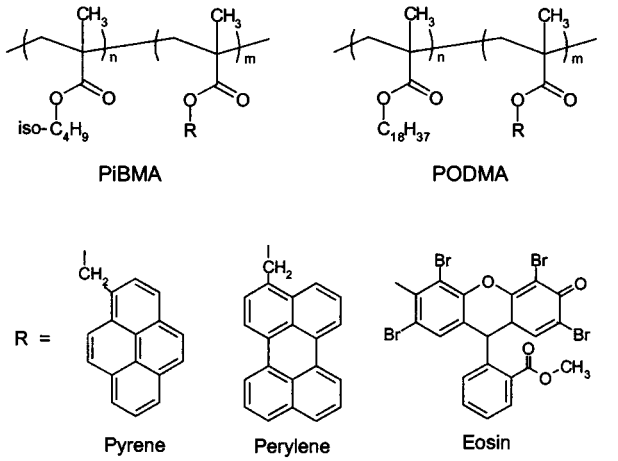

Figure 1. Chemical structures of polymers labeled with fluorescent dyes.

and after annealing was discussed through the excitation energy transfer dynamics among the dyes introduced to PODMA and PiBMA.

Experiments

Sample Preparation. PODMA and PiBMA were labeled at the side chains with fluorescent dye molecules: pyrene (Py), perylene (Pe), and eosin (Eo). The chemical structures are shown in Figure 1. Dye-labeled methacrylates, 1-pyrenylmethyl methacrylate, 3-perylenylmethyl methacrylate, and eosin methacrylate were synthesized by the esterification of methacryloyl chloride. 1-Pyrenylmethyl methacrylate was synthesized by the following procedure. 1-Pyrenemethanol was prepared by the reduction of 1-pyrenecarboxaldehyde (Aldrich) with $NaBH_4$. Methacryloyl chloride (Tokyo Chemical Industry) was added dropwise to a THF solution of 1-pyrenemethanol and pyridine at 0 °C and then stirred for 3 h at room temperature. The product was purified by twice recrystallization from ethanol. 3-Perylenylmethyl methacrylate was prepared from 3-perylenemethanol, which was synthesized by the reduction of 3-formylperylene following the Vilsmeiyer reaction of perylene. Eosin-labeled methacrylate monomer was synthesized by the esterification of methacryloyl chloride with methyl eosin (Aldrich) in DMF. PiBMA labeled at the side chains was prepared by the copolymerization of isobutyl methacrylate (distilled under reduced pressure, Nacalai Tesque) and one of the dye-labeled methacrylate monomers. Polymerization was carried out by the free radical polymerization initiated by α, α′-azobisisobutyronitrile (Nacalai Tesque) in toluene at 60 °C for 24 h. PODMA was polymerized from octadecyl methacrylate (recrystallized from acetone, Tokyo Chemical Industry) in the same manner as PiBMA. Polymers were purified by the repeated reprecipitation from toluene into methanol. Molecular weight was determined by size exclusion chromatography calibrated with polystyrene standards. The fraction of fluorescent moiety, *f*, introduced into the polymer chain was estimated from UV−vis absorption (U3500, Hitachi) and 400 MHz ^{1}H NMR (JNM-EX400, JEOL) measurements. Characterization of the sample polymers is summarized in Table 1.

A mixed benzene solution of dye-labeled PiBMA and PODMA (0.1 g L^{-1}) was dropped onto the surface of pure water, which was ion-exchanged, distilled, and treated with a water purification system (Nano Pure II, Barnstead). The composition of PODMA/PiBMA mixture was 1:1 by the monomer unit. The subphase temperature was kept at 20 °C when spreading the polymer solution. After evaporation of the solvent, the temperature of the subphase was raised to 40 °C and kept constant for a given duration to anneal the monolayer and then lowered to 20 °C. The monolayer was compressed up to 5 mN m^{-1} and then transferred onto a clean cover slip by the vertical dipping method at a rate of 2.0 mm min^{-1}.

TABLE 1: Characterization of Polymers

	$M_n/10^3$	M_w/M_n	*f*/%
PODMA−Pe	11.9	2.08	2.0
PODMA−Py	14.4	1.94	2.3
PiBMA−Pe	45.1	1.56	2.0
PiBMA−Py	39.6	2.05	2.9
PiBMA−Eo	48.8	1.50	2.5

Measurements. The SNOM system used in this study was based on a commercially available instrument (SP-301, Unisoku). A CW He−Cd laser (λ = 325 and 442 nm; IK5351R−D, Kimmon Electric) and the second harmonic of a picosecond Ti:Sapphire laser (λ = 415 nm; Tsunami, Spectra Physics) were used as the light sources. Commercially available SNOM probes cannot be used for the UV excitation because of the low transmittance and the autofluorescence of the optical fiber core in the UV region. The SNOM probes were made from an optical fiber with a pure silica core by etching in a hydrogen fluoride solution buffered with NH_4F following a heating-and-pulling process (P-2000, Sutter Instrument).[15,24] The cone angle and the radius of curvature at the end of a tip were ca. 60 ° and less than 25 nm, respectively. Then, except for the tip end, the side of the probe was metal-coated to prevent the light leakage. The diameter of the aperture was typically 50−100 nm, which was confirmed by scanning electron microscopy. Autofluorescence from the optical fiber core was negligible when the 325 nm line of the He−Cd laser was coupled in. Thus, the use of homemade probes made of a pure silica enabled us to carry out SNOM measurements in the UV region. The distance between the probe and the sample surface was regulated to be several nanometers by a shear force feedback system. The fluorescence from the sample was collected by a high NA objective (1.3 NA, Nikon) and detected with a photomultiplier (R4220P, Hamamatsu Photonics). Time-resolved measurement was carried out by the time-correlated single photon counting method.[25] The fwhm of the instrumental response function was ca. 500 ps. All measurements were carried out at room temperature.

Results and Discussion

Phase Separation Structure Before Annealing. Figure 2a,b shows the perylene and pyrene fluorescence SNOM images for the same area of a PODMA−Pe/PiBMA−Py monolayer deposited without annealing process, respectively. These images have complementary features. This indicates that the phase-separated polymer monolayer could be transferred on a substrate without any defect. It is known that the energy transfer from pyrene to perylene, used as fluorescent dyes in this sample, occurs efficiently when these molecules are at a distance of several nanometers because the Förster radius for the pyrene−perylene pair is 3.3 nm and the energy transfer efficiency steeply decreases with the increase in the separation distance between the donor and the acceptor.[26] Since the emission bands for pyrene and perylene are clearly separated from each other, the combination of pyrene and perylene is suitable for the energy transfer fluorescence imaging. Figure 2c shows the energy transfer SNOM image obtained by collecting the perylene fluorescence under the selective excitation of pyrene at 325 nm. Comparison of the energy transfer image in Figure 2c with

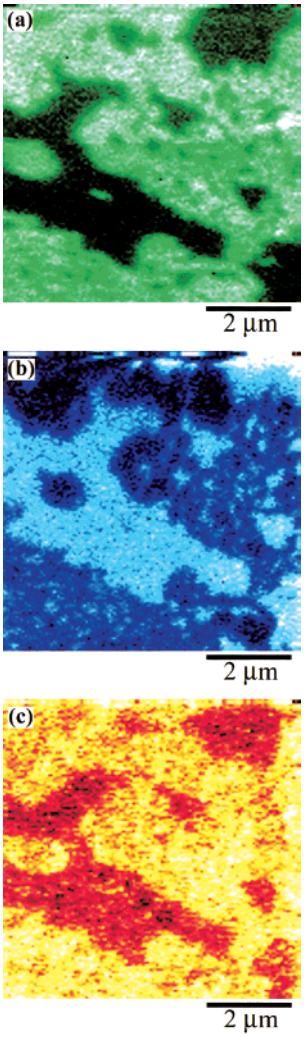

Figure 2. Fluorescence SNOM images for the phase-separated PODMA−Pe/PiBMA−Py monolayer before annealing. (a) Perylene fluorescence image. The excitation wavelength was 442 nm, and the fluorescence from perylene was collected. (b) Pyrene fluorescence image. The excitation wavelength was 325 nm. A filter, UV-D33S (Toshiba), was placed in front of the detector to collect only the fluorescence from pyrene (360−400 nm). (c) Energy transfer SNOM image. The perylene fluorescence was recorded with the selective excitation of pyrene at 325 nm.

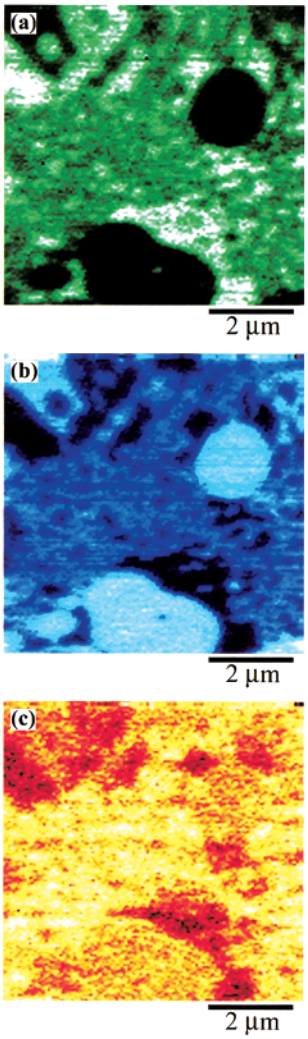

Figure 3. Perylene (a), pyrene (b), and energy transfer (c) fluorescence SNOM images for the PODMA−Py/PiBMA−Pe monolayer before annealing. The measurement conditions were the same as those for the PODMA−Py/PiBMA−Pe monolayer (Figure 2).

Figure 2a,b revealed that the location of the bright area where energy transfer emission took place was in good agreement with the position of the PODMA−Pe rich domain.

The same measurements were carried out for a PODMA−Py/PiBMA−Pe blend monolayer, for which the polymer−dye combination was opposite to that of the PODMA−Pe/PiBMA−Py sample. The SNOM images for the PODMA−Py/PiBMA−Pe monolayer are shown in Figure 3. Similarly to the previous PODMA−Pe/PiBMA−Py sample, the perylene fluorescence image is a negative copy of the pyrene fluorescence image and vice versa. The perylene fluorescence SNOM image has three distinct intensity levels: low, intermediate, and high fluorescence intensities. The dark and bright areas are attributed to the PODMA−Py and PiBMA−Pe domains, respectively. The AFM study for the PODMA/PiBMA blend monolayer showed that a part of the PODMA domains had a network structure including PiBMA chains on a scale of 100 nm.[11] The area with the intermediate intensity probably corresponds to such a network-like domain, from which the observed intensity appeared uniform because the structure size was smaller than the resolution of SNOM. Comparing the energy transfer emission image (Figure 3c) with the perylene and pyrene fluorescence images (Figures 3a and 3b), it was again found that the fluorescence due to the energy transfer was preferentially detected from the PODMA rich domain and not from the PiBMA domain.

The spatially resolved energy transfer measurement by SNOM provides further insight into the phase separation structure of the polymer blend monolayer; that is, the energy transfer fluorescence SNOM image directly indicates the coexistence of PODMA and PiBMA. As shown in Figures 2c and 3c, for both PODMA−Pe/PiBMA−Py and PODMA−Py/PiBMA−Pe monolayers without annealing, the energy transfer occurred in the PODMA rich domain irrespective of the polymer−dye combination. This result indicates that the PODMA rich domain includes the other component, PiBMA. Since the octadecyl side chains of PODMA crystallize at room temperature,[27] PODMA aggregates and forms a solidlike monolayer in spreading the polymer blend solution onto a water surface. The strong cohesive interaction between the long alkyl side chains of PODMA resulted in the domain formation before the phase separation of PODMA and PiBMA was completed. Consequently, the PiBMA components were trapped in the PODMA domain, yielding the energy transfer emission. Since the PiBMA

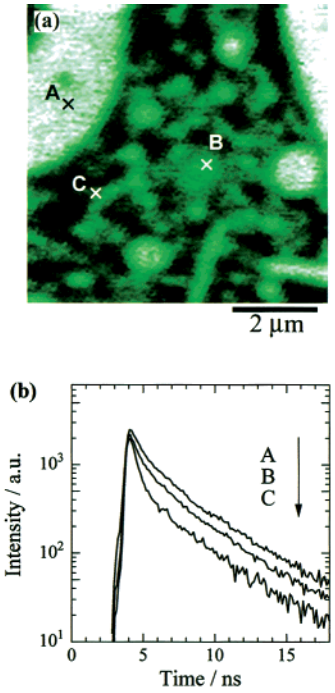

Figure 4. Perylene fluorescence SNOM image for the PODMA−Pe/PiBMA−Eo monolayer deposited without annealing (a) and fluorescence decay curves obtained at the different probe positions (b). The excitation wavelength was 415 nm, and the fluorescence from perylene (460−500 nm) was collected through appropriate filters.

monolayer is liquidlike, it is unlikely that a small amount of PODMA is isolated within the PiBMA domain. Therefore, the energy transfer emission was detected preferentially from the PODMA rich domains and not from the PiBMA domain.

The near-field time-resolved measurement was also carried out for the phase-separated monolayer. In the fluorescence decay measurements, the PODMA−Pe/PiBMA−Eo blend monolayers were used as the samples. Eosin is an energy acceptor for perylene, and the Förster radius for perylene−eosin pair was evaluated to be 4.0 nm from a separate experiment.[28] The perylene fluorescence SNOM image is shown in Figure 4a. The eosin fluorescence image could not be obtained due to the low quantum yield for the fluorescence of PiBMA−Eo. The phase separation structure was similar to those for the PODMA−Pe/PiBMA−Py and PODMA−Py/PiBMA−Pe monolayers irrespective of the polymer−dye combination. This implies that the introduction of a small amount of dye molecules (2−3% of the side group) had little influence on the phase separation structure. The near-field fluorescence decay curves were obtained at the different points denoted as A, B, and C in Figure 4a. Each decay curve is depicted in Figure 4b. The brightness in Figure 4a indicates the "area" fraction of PODMA−Pe; the brighter perylene fluorescence intensity is at a given area, the larger the fraction of PODMA−Pe will be. Figure 4b shows that the perylene fluorescence decays faster with the decrease of the PODMA−Pe fraction, i.e., with the increase of the PiBMA−Eo fraction, because the eosin molecules deactivate the excited perylene through the energy transfer mechanism. Thus, the near-field fluorescence decay curve reflects the polymer fraction at a local area pointed by the fiber probe.

Annealing Process. Figure 5 shows the fluorescence SNOM images for the PODMA−Pe/PiBMA−Py monolayers with different annealing times, t_{anneal} = 0, 5, and 60 min, prior to deposition onto substrates. These images were obtained by illuminating the optical near field at a wavelength of 442 nm

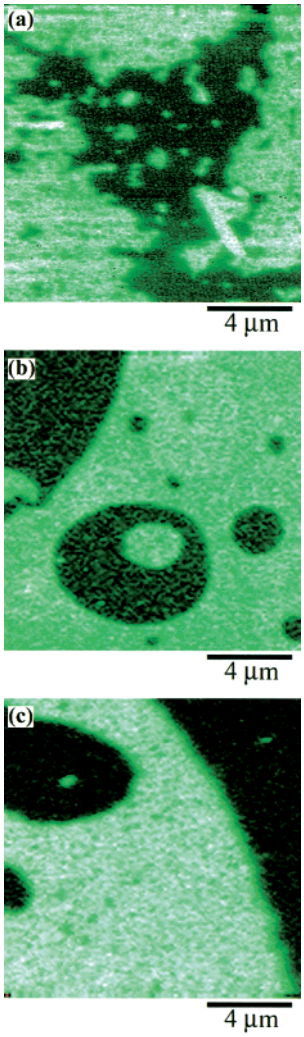

Figure 5. Perylene fluorescence SNOM images for the PODMA−Pe/PiBMA−Py monolayers with different annealing times: (a) 0, (b) 5, and (c) 60 min. The excitation wavelength was 442 nm, and the fluorescence from perylene was collected through a filter, SC-46 (Fuji).

and collecting the fluorescence of perylene. The bright areas correspond to the PODMA rich domains, which were labeled with perylene. Figure 5a indicates the image of the phase separation structure for t_{anneal} = 0 min, i.e., deposited without annealing. The domain shape for the monolayer before annealing was indented, and the domain size had a broad dispersion from ∼100 nm to several tens of micrometers. Figure 5b,c shows the SNOM micrographs for the monolayers annealed at 40 °C. The structure of the phase-separated monolayers after annealing was round-shaped and large compared to that before annealing (Figure 5a). The structure for t_{anneal} = 60 min was larger than that for t_{anneal} = 5 min. Π-A isotherm measurements[27] and BAM[11] have shown that the octadecyl side chain melts at 32−33 °C at the air/water interface. The PODMA behaves as a liquidlike monolayer at the annealing temperature of 40 °C. Consequently, PODMA and PiBMA become further separated from each other because of the incompatibility of these polymers. Thus, the phase separation of the PODMA/PiBMA monolayer proceeds by annealing on a water surface. The polymer composition in each phase reached the equilibrium within several minutes (Figure 5a,b), and then the size of the structure increased with the annealing period (Figure 5b to 5c).

Phase Separation Structure After Annealing. The phase separation structure of the PODMA−Pe/PiBMA−Py monolayer

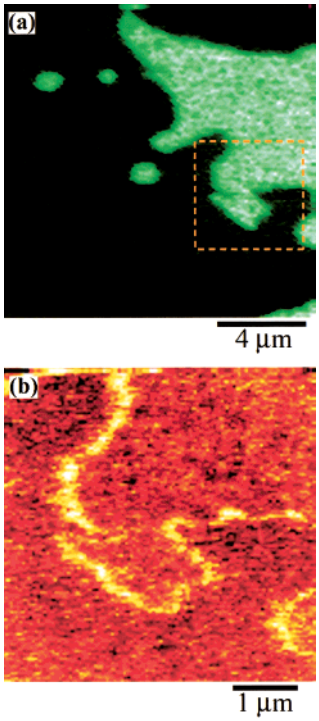

Figure 6. Perylene fluorescence (a) and energy transfer emission (b) SNOM images of the PODMA−Pe/PiBMA−Py monolayer after annealing. Panel b was obtained by scanning the area indicated as a dashed square in panel a.

annealed at 40 °C is discussed through the energy transfer SNOM measurements. As shown in Figure 6, only the phase boundary was measured as a bright area in the energy transfer SNOM image. The width of the fluorescent region was estimated to be 100−300 nm from Figure 6b.

The time-resolved fluorescence measurements were carried out in order to examine the structure of the phase boundary region in more detail. Figure 7a depicts the fluorescence image for PODMA−Pe/PiBMA−Eo after annealing for 60 min. The fluorescence decays for perylene were obtained across the phase boundary. The obtained fluorescence decays were fitted to a three-component exponential function, eq 1, convoluted with the instrumental response function

$$S(t) = S_0\left[a_1 \exp\left(-\frac{t}{\tau_1}\right) + a_2 \exp\left(-\frac{t}{\tau_2}\right) + a_3 \exp\left(-\frac{t}{\tau_3}\right)\right] \quad (1)$$

where S_0 is the intensity at $t = 0$ and $a_1 + a_2 + a_3 = 1$. The mean fluorescence lifetime, $\langle\tau\rangle$, was evaluated by the following equation:

$$\langle\tau\rangle = S_0^{-1}\int_0^\infty S(t)\,dt = a_1\tau_1 + a_2\tau_2 + a_3\tau_3 \quad (2)$$

Figure 7b shows the fluorescence lifetime and intensity profiles along the line A indicated in Figure 7a. The mean lifetime of perylene fluorescence decreased gradually at the phase interface with scanning of the probe from the POMDA−Pe to PiBMA−Eo domains. The alteration of the lifetime was observed for the region of 200−400 nm in width. The effect of the SNOM probe on the time-resolved measurement is considered. Xie et al. reported that the fluorescence lifetime of a single dye molecule on a substrate was perturbed by the metal coating of the SNOM probe.[29,30] However, in our case, the fluorescence lifetime was almost constant irrespective of the distance between the probe and the sample surface. This implies that there is little effect of the SNOM tip upon the fluorescence decay profile. Although the fluorescence decay for the PODMA−Pe monolayer by the near-field excitation deviated from a single exponential function, this was probably due to the other factors. Therefore, it is safely said that the alteration of the fluorescence lifetime across the phase interface resulted from that of the energy transfer rates at the local area under the near-field aperture. To discuss the effect of the interfacial width on the lifetime profile, we carried out a computer simulation.

Simulation of the Fluorescence Lifetime Profile. The perylene fluorescence decay was calculated according to the simplified model which assumed (1) random dye distribution in a plane, (2) no perturbation of the metal coating on the tip to the energy transfer mechanism, and (3) homogeneous distribution of the optical near field emanating from the aperture, i.e., uniform excitation probability for all dyes under the aperture. As mentioned above, the tip effect on the fluorescence lifetime was almost negligible in our experiment. Therefore, the lifetime alteration with the position of the phase boundary can be simulated according to the following procedure. (i) Perylene and eosin molecules were dispersed in a two-dimensional plane assuming that PODMA−Pe and PiBMA−Eo domains come into contact at the boundary of W nm in width, i.e., the plane densities of perylene and eosin at position x, $d_{Pe}(x)$, and $d_{Eo}(x)$, were given as the following equations:

$$d_{Pe}(x) = \sigma_{Pe}P(x) \quad (3)$$

$$d_{Eo}(x) = \sigma_{Eo}(1 - P(x)) \quad (4)$$

$$\begin{aligned} P(x) &= 1 && \text{for } x < -W/2 \\ &= \frac{1}{2} - \frac{x}{W} && \text{for } -W/2 \le x \le W/2 \\ &= 0 && \text{for } x > W/2 \end{aligned} \quad (5)$$

where σ_{Pe} and σ_{Eo} are the plane densities of the pure PODMA−Pe and PiBMA−Eo domains, respectively. $d_{Pe}(x)$ and $d_{Eo}(x)$ are schematically illustrated in Figure 8a. (ii) The probe position, x, was determined, and then the perylene and eosin molecules under the aperture were counted. (iii) The fluorescence decay curve for one perylene molecule under the aperture, $S_I(t;x)$, was estimated according to

$$S_I(t;x) = \exp\left[-\frac{t}{\tau_0}\left\{1 + \sum_j\left(\frac{R_0}{r_{Ij}}\right)^6\right\}\right] \quad (6)$$

where τ_0, R_0, and r_{Ij} are the fluorescence lifetime without quenching processes, the Förster radius, and the distance between Ith perylene and jth eosin, respectively. For all the perylene molecules under the probe aperture, the calculations were carried out. (iv) The fluorescence decay with the SNOM probe located at position x, $S(t;x)$, was calculated as the sum of the decay curves for perylene molecules under the aperture. The detailed calculation procedure for steps iii and iv is described elsewhere.[31,32] (v) The calculations ii−iv were carried out with respect to the different probe positions. Finally, the fluorescence lifetime at each probe position was obtained according to eq 2. Thus, the fluorescence decays with a line scan across the phase boundary were obtained for a given dye distribution. In this calculation, the aperture diameter was assumed to be 100 nm,

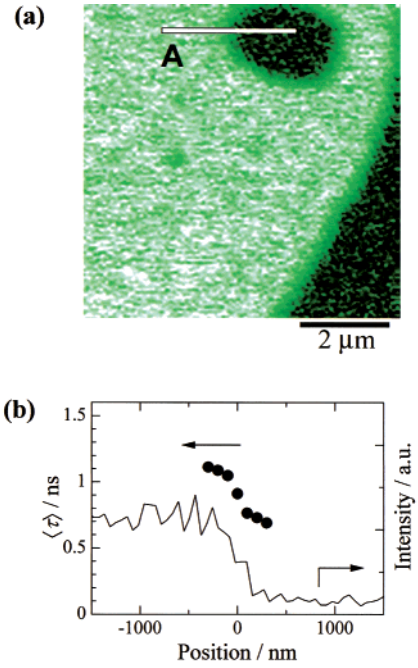

Figure 7. Perylene fluorescence SNOM image for the PODMA−Pe/PiBMA−Eo monolayer annealed for 60 min at the air/water interface prior to deposition (a) and fluorescence lifetime and intensity profiles (b). The excitation wavelength was 415 nm. The closed circles and the solid line in panel b indicate the lifetime and the intensity measured along the line A in panel a, respectively. The lifetime was evaluated by fitting the obtained decay curve to a three-component exponential function.

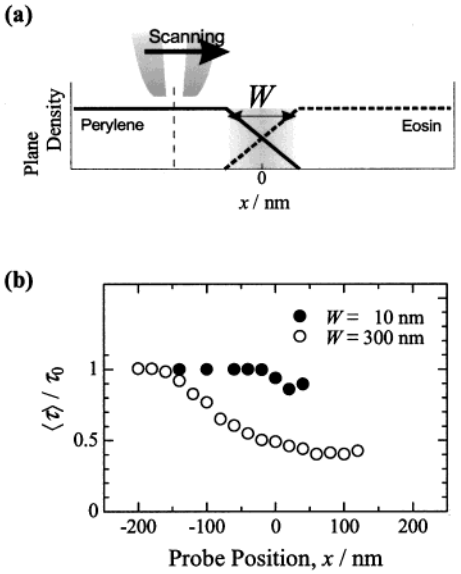

Figure 8. Schematic illustration for the distribution of perylene and eosin molecules (a) and calculated perylene fluorescence lifetime profiles across the boundary region (b). Closed and open circles in panel b indicate the data for $W = 10$ and 300 nm, respectively.

and the other parameters, such as σ_{Pe}, σ_{Eo}, and R_0, were obtained from separate experiments.

The decay curves calculated for $W = 10$ and 300 nm are shown in panels a and b of Figure 9, respectively. For the narrow boundary ($W = 10$ nm), the calculated intensity, $S(0;x)$, decreased with scanning the aperture toward the PiBMA−Eo domain. At the boundary region, the number of the perylene molecules beneath the aperture varied with scanning, which was

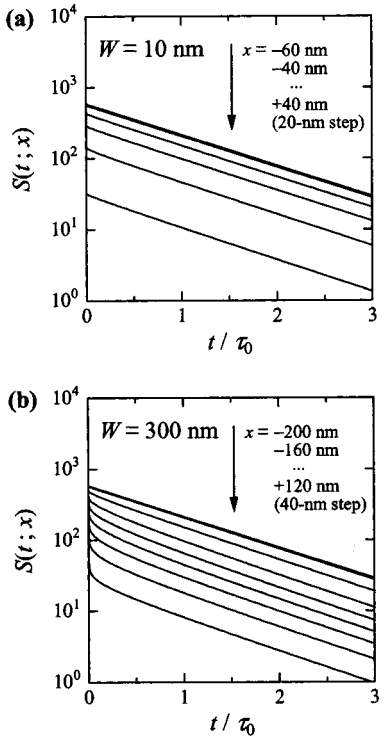

Figure 9. Calculated perylene fluorescence decay curves with scanning the aperture from PODMA−Pe to PiBMA−Eo domains across the phase interface. The decays were calculated for $W = 10$ nm (a) and $W = 300$ nm (b).

directly correlated to the emission intensity. On the other hand, it should be noted that the calculated fluorescence decay profile was independent of the probe position, whereas the intensity changed at the interface. This is clearly shown in the line scan of the calculated lifetime for $W = 10$ nm in Figure 8b (closed circle). As mentioned above, the excitation energy transfer occurs only in the boundary region. In the case of $W = 10$ nm, because the interface was narrow compared to the aperture diameter, most of the excited perylene molecules under the probe were not in the boundary region and emitted fluorescence with the intrinsic lifetime, τ_0, without energy transfer. Therefore, the fluorescence decay profile was independent of the probe position.

In contrast to the case of the narrow interface, the fluorescence decay profile for the wide boundary region, $W = 300$ nm, was dependent upon the aperture position. At the phase boundary, the fluorescence decay profile deviated from the intrinsic profile for perylene as depicted in Figure 9b, and the deviation became greater with scanning the probe. The fluorescence lifetime gradually decreased with scanning the aperture toward the PiBMA−Eo domain. The simulated lifetime line scan is indicated by open circles in Figure 8b. In this case, the aperture size was smaller than the phase boundary. Consequently, the fluorescence lifetime was dependent on the probe position around the phase interface between two domains. Thus, the alteration of the mean fluorescence lifetime was observed only when the interfacial width is comparable to or larger than the aperture diameter.

The experimental result obtained from the time-resolved SNOM measurement was in good agreement with the fluorescence lifetime profile calculated for the wide interfacial width. Although the width of the phase boundary cannot be discussed quantitatively from the calculation presented here, the good agreement about the lifetime profiles obtained by the experiment

and the calculation indicates clearly that PODMA and PiBMA were actually mixed in the molecular scale at the boundary on the order of a few hundred nanometers in width. The interface thickness for PODMA/PiBMA in the three-dimensional bulk state was estimated to be ca. 3 nm[23] from the theoretical equation derived by Helfand and co-workers[33,34] using the calculated interaction parameter.[35] The interfacial width for the PODMA/PiBMA blend monolayer was considerably larger than the estimated thickness for bulk state. Such a large difference probably resulted from the low degree of freedom for the two-dimensional polymer chain.

Conclusion

The phase separation behavior of PODMA/PiBMA blend monolayers was investigated by scanning near-field optical microscopy (SNOM). For the monolayer without annealing, a small amount of PiBMA component was incorporated within the PODMA rich domain. This is due to the strong crystallinity of the octadecyl side chain, which causes quick formation of a solidlike domain before the phase separation is completed. By raising the subphase temperature to 40 °C, the phase separation of both polymers was almost completed in several minutes, and then the domain size increased with annealing time. The fluorescence intensity and lifetime profiles were obtained by time-resolved SNOM measurement for the phase-separated monolayer annealed for 60 min. The alteration of the fluorescence lifetime at the phase interface indicated the existence of the phase boundary on the order of a hundred nanometers, which was fairly wide compared to the interfacial thickness estimated in the bulk state.

Acknowledgment. We would like to thank Prof. Motoichi Ohtsu, Tokyo Institute of Technology, Dr. Shuji Mononobe, and Dr. Toshiharu Saiki, Kanagawa Academy of Science and Technology, for their advice on the probe fabrication. This work was supported by a Grant-in-Aid (No. 10875197 and 12305061) from the Ministry of Education, Science, Sports, and Culture of Japan. H.A. wishes to thank Research Fellowships of the Japan Society for the Promotion of Science for Young Scientists.

Note Added after ASAP Posting

This article was posted ASAP without Figures 2−7 in color on 4/7/01. The corrected version was posted on 4/27/01.

References and Notes

(1) Ito, S.; Ohmori, S.; Yamamoto, M. *Macromolecules* **1992**, *25*, 185.
(2) Mabuchi, M.; Ito, S.; Yamamoto, M.; Miyamoto, T.; Schmidt, A.; Knoll, W. *Macromolecules* **1998**, *31*, 8802.
(3) Taniguchi, T.; Fukasawa, Y.; Miyashita, T. *J. Phys. Chem. B* **1999**, *103*, 1920.
(4) Ohkita, H.; Ishii, H.; Ito, S.; Yamamoto, M. *Chem. Lett.* **2000**, 1092.
(5) de Gennes, P. G. *Scaling Concepts in Polymer Physics*; Cornell University Press: Ithaca, New York, 1979.
(6) Sato, N.; Ito, S.; Yamamoto, M. *Macromolecules* **1998**, *31*, 2673.
(7) Sato, N.; Osawa, Y.; Ito, S.; Yamamoto, M. *Polym. J.* **1999**, *31*, 488.
(8) Hashimoto, T.; Tsutsumi, K.; Funaki, Y. *Langmuir* **1997**, *13*, 6869.
(9) Kumaki, J.; Hashimoto, T. *J. Am. Chem. Soc.* **1998**, *120*, 423.
(10) Sato, N.; Ito, S.; Yamamoto, M. *Polym. J.* **1996**, *28*, 784.
(11) Sakurai, Y.; Sato, N.; Ito, S.; Yamamoto, M. *Kobunshi Ronbunshu* **1999**, *56*, 850.
(12) Yuba, T.; Yokoyama, S.; Kakimoto, M.; Imai, Y. *Adv. Mater.* **1994**, *6*, 888.
(13) Betzig, E.; Trautman, J. K. *Science* **1992**, *257*, 189.
(14) Paesler, M. A.; Moyer, P. J. *Near-Field Optics: Theory, Instrumentation, and Applications*; John Wiley & Sons: New York, 1996.
(15) Ohtsu, M., Ed. In *Near-Field Nano/Atom Optics and Technology*; Springer: Tokyo, 1998.
(16) Hecht, B.; Sick, B.; Wild, U. P.; Deckert, V.; Zenobi, R.; Martin, O. J. F.; Pohl, D. W. *J. Chem. Phys.* **2000**, *112*, 7761.
(17) Hwang, J.; Tamm, L. K.; Bohm, C.; Ramalingam, T. S.; Betzig, E.; Edidin, M. *Science* **1995**, *270*, 610.
(18) Hollars, C. W.; Dunn, R. C. *J. Phys. Chem. B* **1997**, *101*, 6313.
(19) Kerimo, J.; Adams, D. M.; Barbara, P. F.; Kaschak, D. M.; Mallouk, T. E. *J. Phys. Chem. B* **1998**, *102*, 9451.
(20) Mei, E.; Higgins, D. A. *Appl. Phys. Lett.* **1999**, *75*, 430.
(21) Vanden Bout, D. A.; Kerimo, J.; Higgins, D. A.; Barbara, P. F. *Acc. Chem. Res.* **1997**, *30*, 204.
(22) Hofkens, J.; Latterini, L.; Vanoppen, P.; Faes, H.; Jeuris, K.; De Feyter, S.; Kerimo, J.; Barbara, P. F.; De Schryver, F. C. *J. Phys. Chem. B* **1997**, *101*, 10588.
(23) Aoki, H.; Sakurai, Y.; Ito, S.; Nakagawa, T. *J. Phys. Chem. B* **1999**, *103*, 10553.
(24) Mononobe, S.; Saiki, T.; Suzuki, T.; Koshihara, S.; Ohtsu, M. *Opt. Commun.* **1998**, *146*, 45.
(25) O'Cornner, D. V.; Phillips, D. *Time-Correlated Single Photon Counting*; Academic Press: London, 1984.
(26) Berlman, I. B. *Energy Transfer Parameters of Aromatic Compounds*; Academic Press: New York, 1973.
(27) Nakahara, T.; Motomura, K.; Matuura, R. *J. Polym. Sci. A-2* **1966**, *4*, 649.
(28) Aoki, H.; Tanaka, S.; Ito, S.; Yamamoto, M. *Macromolecules* **2000**, *33*, 9650.
(29) Xie, X. S.; Dunn, R. C. *Science* **1994**, *265*, 361.
(30) Bian, R. X.; Dunn, R. C.; Xie, X. S. *Phys. Rev. Lett.* **1995**, *75*, 4772.
(31) Ohmori, S.; Ito, S.; Yamamoto, M. *Macromolecules* **1991**, *24*, 2377.
(32) Mabuchi, M.; Kawano, K.; Ito, S.; Yamamoto, M.; Takahashi, M.; Masuda, T. *Macromolecules* **1998**, *31*, 6083.
(33) Helfand, E.; Tagami, Y. *J. Chem. Phys.* **1972**, *56*, 3592.
(34) Broseta, D.; Fredrickson, G. H.; Helfand, E.; Leibler, L. *Macromolecules* **1990**, *23*, 132.
(35) Krause, S. *J. Macromol. Sci. Rev. Macromol. Chem.* **1972**, *C7*, 251.